Westbrook Cherie J. (Orcid ID: 0000-0003-1666-3979)

Quantifying relative contributions of source waters from a subalpine wetland to downstream water bodies

Hathaway, J.M.[1], Westbrook, C. J.[2], Rooney, R. C.[3], Petrone, R.M.[1], and Langs, L.E.[1,4]

[1] Hydrometeorology Research Group, Department of Geography and Environmental Management, University of Waterloo, 200 University Ave W, Waterloo ON N2L 3G1

[2] Department of Geography and Planning, University of Saskatchewan, 117 Science Place, Saskatoon, SK S7N 5C8

[3] Department of Biology, University of Waterloo, 200 University Ave W, Waterloo ON N2L 3G1

[4] Centre for Hydrology, University of Saskatchewan, Saskatoon, Alberta, Canada

Corresponding Author: Richard Petrone at rich.petrone@uwaterloo.ca

Abstract

Subalpine regions of the Canadian Rocky Mountains are expected to experience continued changes in hydrometeorological processes due to anthropogenically-mediated climate warming. As a result, fresh water supplies are at risk as snowmelt periods occur earlier in the year, and glaciers contribute less annual meltwater, resulting in longer growing seasons and greater reliance on rainfall to generate runoff. In such environments, wetlands are potentially important components that control runoff processes, but due to their location and harsh climates their hydrology is not well studied. We used stable water isotopes of hydrogen and oxygen (δ^2H and δ^{18}O), coupled with MixSIAR, a Bayesian mixing model, to understand relative source water contributions and mixing within Burstall Wetland, a subalpine wetland (1900 m a.s.l.), and the larger Burstall Valley. These results were combined with climate data from the Burstall Valley to understand hydrometeorological controls on Burstall Wetland source water dynamics over spatiotemporal timescales. Our results show that the seasonal isotopic patterns within Burstall Wetland reflect greater reliance on snowmelt in spring and rainfall in the peak and post-growing season periods. We found a substantial degree of mixing between precipitation (rain and snow) and stored waters in the landscape, especially during the pre-growing season. These findings suggest that longer growing seasons in subalpine snow-dominated landscapes put wetlands at risk of significant water loss and increased evaporation rates potentially leading to periods of reduced runoff during the peak- growing season and in extreme cases, wetland dry out.

KEYWORDS: hydrology, meteorology, isotopes, wetlands, subalpine, mixing, runoff, climate

This article has been accepted for publication and undergone full peer review but has not been through the copyediting, typesetting, pagination and proofreading process which may lead to differences between this version and the Version of Record. Please cite this article as doi: 10.1002/hyp.14679

in stream water contribution during the post-growing season potentially correlated with less rain events and inputs from glacial melt water.

The spatiotemporal consistency in source water composition of surface waters generated by MixSIAR allowed for the development of a generalized schematic representation of water movement throughout Burstall catchment during the pre-, peak-, and post- growing seasons (Figure 8). During the pre-growing season, frequent rain events and meltwater inputs trigger rapid streamflow and groundwater recharge resulting in mixing at lake outlet surfaces (Figure 9). As temperatures increase and meltwater (snow) inputs cease during the peak-growing season, rainfall becomes the dominant source water input, and is quickly mobilized upon reaching the surface thus reducing water residence time and allowing for minimal groundwater recharge time (Figure 9). Although rain is the dominant source, total precipitation during August is significantly lower than June (83.2 mm vs. 142.2 mm, respectively), and evaporation is increased due to higher temperatures resulting in lower lake water levels, thus indicating periods of low flow during the peak season. MixSIAR results show that groundwater and stream water are the dominant contributors to downstream water bodies during the post- growing season as precipitation events wane (Figure 7). The swift movement of rainwater to streamflow results in low residence time and minimal groundwater recharge. Increase streamflow during this period is likely supported by a missing low end-member source that is shown in Figure 9. .

Headwater wetlands are often surrounded by complex landscapes characterized by steep terrain and harsh climates. Such complexities present challenges to water resource managers, especially because estimates of source water mixing and contributions to downstream surface waters cannot easily be directly measured (Pu et al., 2013). Fortunately, end-member mixing models parameterized with naturally occurring tracers have proven to be an effective method, used in small-scale catchment studies, to identify the contributions of different components to runoff and evaluate streamflow generation mechanisms (Zhang et al., 2018; Ala-aho et al., 2018; Jin et al., 2012; Maurya et al., 2011; Pu et al., 2013). The modern understanding of both mixing end-members and run-off generation has benefited over the past decades from the increased use of environmental tracers since different tracers may provide different complementary information (Šanda et al., 2014; Wu et al., 2019; Langs et al., 2020). That is, various biogeochemical tracers and stable isotopes can help curb the sources of runoff and their temporal dynamics (Lessels et al., 2016). The results from end-member mixing models can be analyzed to reveal the relative importance of each source water to stimulate water flow both within wetlands and to downstream water bodies. Current knowledge of how relative importance varies as a function of climate may foreshadow potential shifts in source waters in the future and identify how land-use interference impacts mountain wetland hydrologic processes.

The Canadian Rocky Mountains represent a major source of freshwater in North America since they store and distribute water to millions of people across Western Canada and parts of the United States, making them the ideal location to study hydrological processes (Hrach, 2020). The leeward slopes of the Canadian Rockies are littered with subalpine (1300 – 2300 m.a.s.l.) and montane (825 – 1850 m a.s.l.) wetlands, all of which are vulnerable to environmental change due to their location in a high-elevation system and reliance on rain and snow meltwater (Reynolds et al., 2022). This study aims to identify source water contributions and movement to downstream water bodies from a spatiotemporal lens throughout an exemplar subalpine catchment. Two main objectives will be addressed using δ^2H and $\delta^{18}O$ as tracer inputs to a simple 2-component mixing model in a glacier-fed headwater catchment. The objectives are to: I) partition the relative contribution from the subalpine wetland to downstream water bodies using a simple two component mixing model, and II) determine source waters during pre-, peak-, and post- growing seasons.

2. STUDY SITE AND METHODS

2.1 Study Site Description

We used the Burstall Wetland, situated in the Kananaskis region of Alberta on the eastern slopes of the Canadian Rocky Mountains. It was chosen to investigate the relative contribution of different water sources to downstream water bodies because of its position in a glacier-fed headwater catchment. Burstall is a mineral wetland stretching about 1.2 km in length with a peat layer extending 20 cm deep. It is poorly drained, with soils resembling peaty muck (Windell et al., 1986).

The Burstall Valley is a steep, glacially carved valley, approximately 6 km long, with the Robertson Glacier occupying the upper 2.8 km (Moran et al., 2007). Burstall Wetland is positioned at about 1900 m a.s.l. within the low terrain of Burstall Valley (Figure 1). There are four lakes at the terminus of the Wetland in Burstall Valley – Burstall Lake, Lake 1, Lake 2, and finally, Mud Lake (Figure 1). The lakes are fed by precipitation and groundwater inputs, spring snowmelt, and meltwater from the Robertson glacier. The hydrology of the valley is controlled by springtime snowmelt water that feeds into the Spray River and subsequently to the Bow River, the major mountain drainage system in southern Alberta (Moran et al., 2007). The wetland vegetation is dominated by *Carex* spp. and *Salix* spp., characteristic of marshes and fens in Alberta.

Typical of most continental mountain regions in continental locations, the Kananaskis Valley climate is highly variable over space and time. Areas like Kananaskis Valley, positioned on the leeward slopes are susceptible to easterly, upslope storms that act as classical orographic systems, and are most common in the spring (Stewart et al., 1995). The complex terrain of the Kananaskis Valley often results in turbulent mixing of air masses due to influences from secondary moisture sources as they cross over topographic barriers (Moran et al., 2007). At higher elevations, most precipitation occurs as snow, and temperatures fluctuate according to variations in the El Nino Southern Oscillation and Pacific Decadal Oscillation (Whitfield, 2014). During the winter months, precipitation is controlled by orographic systems of two major air masses: the maritime Pacific and the continental Polar (Whitfield, 2014). These storms create a standard elevation relationship (depletion in heavy isotope with altitude), commonly observed on windward slopes (Moran et al., 2007).

-.

Figure 1. Map of Burstall Wetland (A) including sampling locations of groundwater (10) in red, rain (1) in green, snow (1) in orange, stream (2) in blue, and surface (7) in teal. Stream 1 and Stream 2are identified with white arrows. Vegetation survey sites are indicated by white (3) dots. The four lakes, including Upper (Burstall Lake), Middle (Lake 1), Lower (Lake 2), and Mud, are shown and labelled. An approximate outline of the Burstall Wetland is shown in black. The insert picture shows the surrounding area including Calgary and the British Columbia/Alberta border. The study site depicted by a blue star. The elevation profile line in (A) correlates with the profile in (B). The elevations identified on the profile line (A) are also indicated in the profile in (B) to show the rapid drop after Lower Lake (Lake 2). The greater Burstall Valley is shown in (C) with approximate boundaries of all 4 lakes and the Burstall Wetland outlined. The Robertson Glacier, ranging in elevation from 2504 – 2866 m a.s.l. (Scanlon, 2017), is outlined by a black box. The distance between the terminus of the glacier and the beginning of the Burstall Wetland is 3.6 km.

2.2 Methodology

2.2.1 Hydrometric data collection

Basic meteorological data was collected by instrumentation on a tripod positioned 4.15 m above the ground near Burstall Lake (Figure 1). Relative humidity and temperature were measured with a HMP 155 (Vaisala, Finland), as well as rainfall. Rain precipitation was measured at Mud Lake at 2.03m above ground using an Ott Pluvio 400 (Ott Hydromet, Loveland, CO, USA). The time series data of air temperature and relative humidity throughout the 2019 and 2020 growing seasons are provided in Figure 2.

Figure 2. Precipitation (mm) plotted from Mud Lake for 2019 and 2020. Air temperature (°C) and relative humidity (%) data plotted from Burstall Wetland for 2019 and 2020 growing season (May-September) shown in 'Day of Year' format.

2.2.2 Isotopic Sample Collection

Potential source waters, including groundwater, rain, snow, stream- (Stream 1 and Stream 2), and surface- waters were sampled for analysis of δ^2H and δ^{18}O. Stream 1 and Stream 2 run through Burstall Wetland and are visually distinct (e.g., different color and location), potentially coming from different sources, and so were sampled separately to provide insights into their origins. A summary of δ^2H, δ^{18}O, and d-excess statistics are shown in Table 1. Water samples were collected during pre- (29 May to 20 July), peak- (21 July to 23 August), and post (24 August to 2 October) growing seasons from May-September in 2019, and during August and September in the 2020 season due to COVID-related access restrictions. Water samples were collected into 20 mL scintillation poly-seal vials with foil lined caps such that the sample contained no headspace. Vials were stored at room temperature (never refrigerated or frozen to limit phase changing) before processing. The pre-, peak-, and post- growing season time periods were determined based on personal observations and field measurements by Hrach (2021) from a subalpine meadow (2083 m a.s.l.) in Kananaskis Country.

Groundwater wells were hand installed at Burstall Wetland to better understand groundwater movement throughout the wetland, and to quantify the relative contribution of groundwater to downstream water bodies. A total of 11 wells were installed; one near the meteorological (MET) tower (Figure 1) at the beginning of the 2019 growing season, and the rest were installed at the end of the 2019 growing season and were sampled during 2020 from August - September. Wells were positioned to best capture the isotopic composition of groundwater near Stream 1 and Stream 2, in addition to various ground cover types. Wells were constructed using Schedule 40 PVC pipe slotted along the entire buried length and extended 1 m below ground. Fabric 2" diameter well sock (ESP Well Supply, USA) was used to cover the outside surface and act as a screen for fine sediments. During the 2019 field season, groundwater was sampled starting in May during the snowmelt period and lasted throughout the growing season (May-September). Sampling procedures consisted of purging the entire well volume three times before collecting the water sample for stable isotope analysis.

Cumulative rain samples were collected monthly at the Burstall Wetland throughout the 2019 growing season and at the end of the 2020 season. The rain collector was positioned near the MET tower (Figure 1). Rain collectors were built to collect and limit evaporation of samples between sampling periods (Groning et al., 2012). A plastic hose was watertight sealed to the bottom of a funnel, which was then sealed to the top of a water reservoir container. The hose was cut with enough length to coil on the bottom of the reservoir to ensure the water level of the collected samples topped over the house, limiting evaporation and phase changing of the sample. A ping-pong ball was placed in the top of the funnel to further limit evaporation.

Snow samples were collected for pre- and post- growing season sampling periods when it was present in 2019. Samples were collected using a plastic bag and then were left to melt at room temperature to ensure complete mixing and no phase change before being sub-sampled into 20 mL poly-seal sampling bottles. The snow was never deep enough to take snow cores, so this method was not used. Snow water samples were only collected during the pre- growing seasons on 5 June and 24 June2019, within a 24-hr of the snowstorms. No samples were collected during the 2020 growing season.

Stream samples were collected throughout the 2019 growing season (May-September) at the Burstall Wetland from Stream 1 and Stream 2, both had water flowing throughout the entire season. Stream 1runs through the center of the wetland and consists of clear water during the early summer months, then transitions to cloudy, turbid water during the late summer months. The secondary stream, referred to as Stream 2, is located on the eastern side of the wetland, consists of reddish-brown water, and experiences low flow throughout the growing season. All 2020 stream samples were collected during the post- growing season (August-September). Samples were taken by dipping uncapped vials into streams facing against the current to ensure minimal hand contact with water sample. Samples were immediately sealed to minimize evaporation.

Surface water samples were collected during September of 2020 at each of the four lakes (Burstall Lake, Lake 1 Outlet, Lake 2 Outlet, and Mud Lake) and Burstall Lake Outlet to measure movement of source water from one lake to the next. Samples were collected using the same methods described for stream water collection.

All water samples were submitted and processed by the Environmental Isotope Laboratory (EIL) at the University of Waterloo, Ontario, using the $\delta^{18}O$ and $\delta^{2}H$ LGR-OA-ICOS Laser System (LGR, 2010; Berman et al, 2013). Maximum analytical uncertainties are ± 0.1‰ for $\delta^{18}O$ and ± 2‰ for $\delta^{2}H$. Quality control was maintained by running a range of water standards including VSMOW (Vienna Standard Mean Ocean Water) and VSLAP (Vienna Standard Light Antarctic Precipitation) from the International Atomic Energy Agency (IAEA). Duplicates were run at a minimum of every fifth sample. Each run also included an in-house check standard for QA/QC of each individual sample batch. Electric conductivity was assumed to be in normal range due to past measurements in the area.

2.2.3 MixSIAR Bayesian Mixing Model

To partition relative source water contributions from Burstall Wetland to downstream water bodies, the R package MixSIAR, a Bayesian mixing model that runs the Markov Chain Monte Carlo (MCMC) method developed by Stock and Semmens (2016), was used. MixSIAR unifies the existing set of mixing model parameterizations into a customizable tool that is designed to analyze biotracer and isotope data to determine relative properties of a mixture and its sources (Stock and Semmens, 2016). The outputs used in this study were summary statistics, which consist of relative contribution percentages and standard deviations, and posterior density plots, which represent the distribution of Bayesian estimated proportions of Burstall Wetland source waters in downstream lakes. Bayesian mixing models improve upon simpler linear mixing models by explicitly taking into account uncertainty in source values, categorical and continuous covariates, and prior-information (Stock and Semmens, 2016). For this study, the script version of MixSIAR was used as the sampling design was a repeated analysis and the MCMC chain lengths could be set. MixSIAR was selected over other mixing model software because of its ability to incorporate covariate data to explain variability in the mixture proportions via fixed and random effects. Different from other Bayesian mixing models, MixSIAR clearly defines and explains the assumed error structures. For the purposes of this study, 'resid_err' was consistently used to account for unexplained deviations from the mean (Stock and Semmes, 2016). MixSIAR assumes mixture values are from a normal distribution, defined by the same mean, with the variance stemming from a combination of source variances (Stock et al., 2018).

Five separate model runs were completed, with 3 runs per model, to analyze the combined effects of season and spatial location at different points throughout the catchment. All source waters (groundwater, rain, stream, and snow) were included in the pre- growing season models runs, then only available source waters (groundwater, rain, and stream) were included in the peak- and post- growing season model runs. To determine the relative contribution of total Burstall Wetland stream water, Stream 1 and Stream 2 data were combined and input as one source, "Stream", into the MixSIAR model. For consistency, each model run had spatial location set as a 'fixed' variable and the time of season was considered a 'random' variable. The run length of the MCMC was set to 'normal' (chain length = 100,000, burn=50,000, thin=50, chains=3). MCMC was used to converge on the posterior distributions of all the variables in the model. It was essential to determine that the model had converged before accepting the output of MixSIAR. Gelman-Rubin and Geweke diagnostic tests were used to determine whether the model was close to convergence (Stock and Semmens, 2013). Both the tropic enrichment factor and concentration dependence were set to zero.

2.2.4 Vegetation Surveys

The ground cover at Burstall Wetland is spatially diverse and appears to vary depending on proximity to a water body (stream or lake). For the purposes of this study, only the four most abundant ground cover species were used to characterize wetland vegetation distribution, the remaining ground cover is identified as "other". Ground cover surveys were carried out across three 50 m transects near the MET tripod (Figure 3). The transects were positioned 50 m apart and trended E-W. Along the transects, five 1x1 m plots were positioned 10 m apart. The percent coverage of all ground cover types was visually estimated for each plot.

2.2.5 Data Analysis

Craig 1961 established that seasonal and climatically driven interactions between the δ^2H and δ^{18}O content of water in precipitation results in a Local Meteoric Water Line (LMWL), which can be linked to water sources to assess the relative importance of seasonal precipitation contribution to regional surface waters. Linear deviations from the LMWL, referred to as the Local Evaporation Line (LEL), are a result of evaporation of surface water that enriches the heavy oxygen and hydrogen content of remaining water. The LEL can be used to provide basin-scale estimates of the degree of evapotranspiration (ET) and water inflow to individual water bodies. The slope of the LEL reflects the influence of varying local conditions (temperature, relative humidity, wind speed, etc.) naturally integrated over the evaporative season.

The Local Meteoric Water Line (LMWL) and Local Evaporation Line (LEL) used in this study were developed by Katvala et al. (2008) using the isotopic composition of precipitation samples. Samples were collected from the Kananaskis Field Station and the University of Calgary Weather Research Station. The Kananaskis Field Station is located within the foothills at an approximate elevation of 1390 m. The University of Calgary station is located within the Prairies at an approximate elevation of 1110 m. The samples collected from the Katvala et al. (2008) study were analyzed for the isotopic ratios of ^{18}O/^{16}O and ^{2}H/^{2}H in the Isotope Science Laboratory at the University of Calgary.

Deuterium Excess (d-excess) is a tool to measure kinetic fractionation effects and is primarily a function of atmospheric relative humidity, wind speed, and air temperature. D-excess can be thought of as an index of deviation from the Global Meteoric Water Line (GMWL), which has a d-excess value of 10‰. Because of the link to humidity, d-excess values are sensitive to evaporative processes, including whether summer or winter precipitation dominates recharge. Due to the close relationship between δ^{18}O and δD in precipitation, values can reflect different environmental characteristics in precipitation moisture sources,

$$d = \delta^2\mathrm{H} - 8 * \delta^{18}\mathrm{O} \qquad (1)$$

In this study, d-excess was used to interpret evaporative influence across the landscape and identify meteorological factors associated with different moisture sources throughout the growing season.

3. RESULTS

3.1 Vegetation Surveys

Wetland ground cover interferes with the movement of water from rainfall to groundwater, to runoff generation and is therefore important to consider in wetland hydrological studies. Interference may occur through processes such as interception, infiltration, or evapotranspiration, all of which can directly alter δ^2H and δ^{18}O signals from wetland source waters (Le Maitre et al., 1999). Thus, to characterize the groundcover at Burstall Wetland, data from surveys conducted during the summer of 2019 are included to help explain spatiotemporal variation in source water signals.

The dominant ground covers were *Salix planifolia*, *Carex aquatilis*, brown moss, and litter (Figure 3). In this context, litter is defined as dead plant material such as leaves, needles, bark, and twigs. It should be noted, however, that there are distinct patches of *Equisetum hymemale* (horsetail) found only on the eastern edge of the wetland, close to Stream 2.

3.2 Spatiotemporal Isotopic Characteristics of Source Waters

The isotopic composition of source waters to downstream water bodies varied extensively between rain, groundwater, snow, and streams (Stream 1 & Stream 2) throughout the 3 sampling periods (pre-, peak-, post- growing seasons).

Figure 3. Percent cover of the four dominant vegetation types and ground cover at Burstall Wetland shown for three E-W transects. Transect locations are indicated in the map by white lines. The MET tower is included for reference.

All source water data is plotted in Figure 4 against the GMWL, the LMWL, and the LEL. The $\delta^{18}O$ of rain varied the most with values ranging from -16.4‰ to -18.6‰, and a mean (± 1 SD) of -17.6 (± 0.87) ‰. $\delta^{2}H$ value ranged from -123‰ to -140.6‰ with a mean (± 1 SD) of -133.6 (± 7.07) ‰. Rain signals deviated slightly from the GMWL indicating potential differences in source characteristics of moisture, either due to the seasonal change of meteorological conditions over the ocean, or evaporative enrichment in droplets beneath the cloud base.

The $\delta^{18}O$ value of snow water ranged from -19.8‰ to -20.4‰ with a mean (± 1 SD) of 20.0 (± 0.293) ‰. $\delta^{2}H$ ranged from -149.3‰ to -154.1‰ with a mean (± 1 SD) of -151.1 (± 2.61) ‰. Groundwater $\delta^{18}O$ ranged from -17.3‰ to -20.1‰ with a mean (± 1 SD) of -18.7 (± 0.76) ‰. $\delta^{2}H$ value of groundwater ranged from -132.4‰ to -151.1‰ with a mean (± 1 SD) of -141.4 (±

Table 1. Summary statistics of average $\delta^{18}O$, $\delta^{2}H$, and d-excess for all source waters from Burstall Wetland. Table is divided into pre-, peak-, and post- growing seasons.

4.74) ‰. The $\delta^{18}O$ values of the Stream 1 ranged from -18.6‰ to -20.0‰ with a mean (± 1 SD) of -9.5 (± 0.593) ‰. $\delta^{2}H$ ranged from -138.7‰ to -153.6‰ with a mean (± 1 SD) of -146.6 (± 4.98) ‰. The $\delta^{18}O$ values of the Stream 2 ranged from -19.1‰ to -21.2‰ with a mean (± 1 SD) of -20.0 (± 0.29) ‰. $\delta^{2}H$ ranged from 143.2‰ to -156.2‰ with a mean (± 1 SD) of -149.01 (± 5.11) ‰. The slope of the regression lines for groundwater (6.08) and Stream 2 (6.18) were slightly lower than that of the LMWL (7.49), indicating that stream water and groundwater (to a depth of 1 m) endured evaporative impacts. The pre- and peak- growing season groundwater samples plot above and slightly below the GMWL, then only during the post- growing season do some samples cross over the LMWL and become more enriched, suggesting rainfall is an important source for groundwater recharge. The slope of the regression line for Stream 1 (7.95) was slightly higher than that of the LMWL, suggesting minimal evaporative impact or sufficient water input to block the evaporative signal. The overall damped variability among source waters indicates mixing between snowmelt and rainfall with stored waters in the landscape.

Figure 4. Dual isotope plot, depicted by color and shape, of grouped groundwater, rain, snow, and stream (Stream 1 & Stream 2) samples collected at Burstall Wetland during the 2019 growing season (May-September) and 2020 season (August-September) plotted along the GMWL (straight line), LMWL (dashed line), and LEL (dotted line). LMWL and LEL were developed by Katvala et al. (2008).

There was a slight depletion in groundwater $\delta^{18}O$ values from the pre- to peak- growing seasons coinciding with a greater range (Figure 5A). The range of $\delta^{18}O$ values expanded further into the post- growing season, although some values consistently cluster around -19.0 ‰ (Figure 5A). The samples that comprised the enriched portion of the post-growing season boxplot were collected from the wetland edges (Figure 6A). The causation of this trend is likely the cumulative effects of multiple factors: i) a declining water table during the post-growing around the wetland edges season and thus a stronger reflection of rainwater $\delta^{18}O$, and ii) increased surface evaporation due to higher temperatures (Figure 2), longer sunlight exposure, and minimal canopy coverage near the wetland edges.

Both streams exhibited slight enrichment throughout the growing season (Figure 5A), however, stream water measurements were more depleted in heavy isotopes than any of the precipitation or groundwater samples indicating there is likely a missing end-member. The combined stream water trends in Figures 5A & 5B further allude to a missing source water since the distribution of $\delta^{18}O$ of both streams remains relatively consistent throughout the growing season, yet the distribution of the d-excess measurements is much greater and plot higher during the pre- and post- period, suggesting precipitation inputs are not responsible for these trends. Indeed, despite warmer temperatures and decreased precipitation inputs, the average d-excess values of Stream 2 increased throughout the growing season suggesting either evaporative enrichment minimally impacts surface waters under warm and dry conditions or Stream 2 is receiving inputs from another source.

The distribution of groundwater $\delta^{18}O$ and d-excess signals varied significantly both seasonally and spatially across Burstall Wetland (Figure 5, Figure 6). Groundwater samples

Figure 5A&B. $\delta^{18}O$ (A) and d-excess (B) distribution boxplot of source waters depicted by color over the pre-, peak-, and post- growing seasons.

collected from the middle of the wetland, where peat is >40 cm thick, were more depleted in $\delta^{18}O$ on average than samples collected from the edges (-19.0‰ and -17.7‰, respectively) (Figure 6A). However, groundwater samples taken from well 3 (Figure 6A) were slightly more depleted in $\delta^{18}O$, which given the proximity to Stream 2 and Burstall Lake, is indicative of mixing between sources towards the mouth of the stream. Samples located near Stream 1had more depleted signatures and greater degree of mixing between groundwater and stream water, which indicates lateral groundwater movement and stream water infiltration (Figure 3).

Regression analysis between d-excess and $\delta^{18}O$ of both streams and groundwater was completed to identify mixing between sources to help elucidate the importance of groundwater to stream flow. The results do not show clear similarities or overlap in the isotopic composition of the streams and groundwater. Indeed, Stream 2 appears more isotopically depleted than

Figure 6A&B. Visual distribution of $\delta^{18}O$ values of groundwater throughout Burstall Wetland (A). From depleted to enriched values; red= -17-17.5‰, orange= -17.6-18‰, yellow= -18.1-18.5‰, green= -18.6-19‰, blue= -19.1-19.5‰, and white= -19.6-20‰. Burstall lake is positioned at the top of the map and then extends southward towards Robertson Glacier. (B) Plot of the deuterium excess versus oxygen -18 for groundwater, Stream 1, and Stream 2 with regression equations and R^2 values shown.

groundwater, suggesting that wetland groundwater (to a depth of 1 m), although it may contribute to Stream 2, is likely not the dominant contributor. Figure (6B) shows moderate correlation between d-excess and $\delta^{18}O$ (r^2=0.65) in groundwater, indicating that depleted $\delta^{18}O$ corresponds to high d-excess values. The depletion of $\delta^{18}O$ values can be visualized in Figure (6A), starting from the edges, and moving to the center of the wetland. There was a weak correlation between $\delta^{18}O$ and d-excess in both Stream 1 & Stream 2 (r^2=0.0021, r^2=0.191, respectively) (Figure 6B). In addition, average d-excess values were higher in streams indicating less evaporation during the late growing season.

3.3 Relative Source Water Contribution and Dominant Flow Regimes of Burstall Catchment

Growing season stage and MixSIAR analysis showed differences across space and time. Although each location had different source water proportions, they all followed similar seasonal trends (Figure 7). All posterior density plots are shown in Figure 8. At Burstall Lake, the proportions of source waters during the pre- growing period are as follows: 25.8% groundwater (SD ± 20.3 %), 48.1% rain (SD ± 22.3 %), 14.6% snow (SD ± 13.3 %), and 11.4% stream (SD ± 10.1 %) (Figure 7). The peak- proportions were 32.0% groundwater (SD ± 21.8 %), 46.5% rain (SD ± 19.3 %), and 21.5% stream (SD ± 15.5 %). Finally, post-season proportions were 37.4% groundwater (SD ± 24.5 %), 13.2% rain (SD ± 9.9 %), and 49
3% stream (SD ± 22.8 %).

For Burstall Lake Outlet the proportions for the pre- growing period are as follows: 25.1% groundwater (SD ± 20.1 %), 54.4% rain (SD ± 22.2 %), 11.6% snow (SD ± 11.3 %), and 9% stream (SD ± 8.5 %). The peak- proportions were 29.4% groundwater (SD ± 20.2 %), 51.8%

rain (SD ± 17.6 %), and 18.8% stream (SD ± 13.2 %). Finally, post-season proportions were 37.3% groundwater (SD ± 24.9 %), 10.2% rain (SD ± 7.6 %), and 52.2% stream (SD ± 22.9 %).

Lake 1 Outlet proportions during the pre- growing period are as follows: 27.1% groundwater (SD ± 20.9 %), 45.8% rain (SD ± 24.8 %), 14.8% snow (SD ± 14.1 %), and 12.2% stream (SD ± 12.1 %). The peak- proportions were 20.9% groundwater (SD ± 18.7 %), 65.6% rain (SD ± 21.1 %), and 13.4% stream (SD ± 12.6 %). Finally, post-season proportions were 41.8% groundwater (SD ± 25.0 %), 22.8% rain (SD ± 12.4 %), and 35.4% stream (SD ± 20.9 %).

Lake 2 Outlet proportions during the pre- growing period are as follows: 23.7% groundwater (SD ± 19.5 %), 58.0% rain (SD ± 22.1 %), 10.4% snow (SD ± 10.4 %), and 7.9% stream (SD ± 8.1 %). The peak- proportions were 24.5% groundwater (SD ± 18.0 %), 59.4% rain (SD ± 15.7 %), and 16.0% stream (SD ± 11.3 %). Finally, post-season proportions were 42.1% groundwater (SD ± 25.4 %), 12.0% rain (SD ± 8.3 %), and 46.0% stream (SD ± 22.5 %).

Lastly, proportions for Mud Lake for the pre- growing period are as follows: 25.8% groundwater (SD ± 20.8 %), 50.6% rain (SD ± 24.4 %), 13.2% snow (SD ± 13.2 %), and 10.4% stream (SD ± 10.8 %). The peak- proportions were 21.8% groundwater (SD ± 18.3 %), 65.0% rain (SD ± 19.9 %), and 13.3% stream (SD ± 11.6 %). Finally, post-season proportions were 42.4% groundwater (SD ± 25.1 %), 19.7% rain (SD ± 11.7 %), and 37.9% stream (SD ± 21.5 %).

Figure 7. Relative source water contribution to downstream water bodies generated by MixSIAR partitioned by sampling period and growing season stage (pre-, peak-, post-).

During the pre-growing period, groundwater and rain precipitation were the most readily mobilized, and together comprised the largest portion of source water contribution to each downstream water body (Figure 7). During the peak-period, rain (45.7%) comprised the largest portion of source water contribution to Burstall Lake, followed by groundwater (32.8%), and stream water (21.6%) ((Figure 7).

Rain was the dominant source water input (51.2%) to Burstall Lake Outlet during the peak-period, controlling surface connectivity between Burstall Lake and Lake 1. Lake 1 Outlet and Mud Lake also saw an increase in rain as the main contributor to source water composition during the peak-growing season (42.5% and 27.8%, respectively) (Figure 7). Rain persisted as the dominant source to Lake 2 Outlet during the peak-growing season, increasing only 0.68%. Groundwater comprised a relatively small portion of surface water at Lake 2 Outlet throughout the growing season, confirming reliance on rainfall and meltwater inputs. There was an increase in stream water contribution during the post-growing season potentially correlated with less rain events and inputs from glacial melt water.

The spatiotemporal consistency in source water composition of surface waters generated by MixSIAR allowed for the development of a generalized schematic representation of water movement throughout Burstall catchment during the pre-, peak-, and post- growing seasons (Figure 8). During the pre-growing season, frequent rain events and meltwater inputs trigger rapid streamflow and groundwater recharge resulting in mixing at lake outlet surfaces (Figure 9). As temperatures increase and meltwater (snow) inputs cease during the peak-growing season, rainfall becomes the dominant source water input, and is quickly mobilized upon reaching the surface thus reducing water residence time and allowing for minimal groundwater recharge time (Figure 9). Although rain is the dominant source, total precipitation during August is significantly lower than June (83.2 mm vs. 142.2 mm, respectively), and evaporation is increased due to higher temperatures resulting in lower lake water levels, thus indicating periods of low flow during the peak season. MixSIAR results show that groundwater and stream water are the dominant contributors to downstream water bodies during the post- growing season as precipitation events wane (Figure 7). The swift movement of rainwater to streamflow results in low residence time and minimal groundwater recharge. Increase streamflow during this period is likely supported by a missing low end-member source that is shown in Figure 9. .

igure 8. Density and proportion spread plots of source water contribution to downstream water bodies generated by MixSIAR for time of growing season (pre-, peak-, post-).

Figure 9. Conceptual model of water movement throughout Burstall Wetland during the pre-, peak-, and post-growing season based on results from MixSIAR (Figure 7). The red "X" in the Peak- growing season frame indicates no infiltration of rainwater to groundwater. The "+" symbol indicates either a positive input or an increase in intensity. The "-" symbol indicates a decrease in intensity or relative contribution. "GW" refers to groundwater. "MW" refers to snow meltwater.

4. DISCUSSION

Subalpine wetlands are important elements of mountain hydrologic systems as contributors to downstream water bodies, but due to their remote nature and harsh climate, their hydrology is not well studied. This research addressed the importance of wetlands in mountain hydrologic systems as potential contributors to downstream water bodies, and the processes that influence them across spatiotemporal scales. We applied stable isotope modeling techniques to partition the relative contribution of source waters from the subalpine wetland to downstream water bodies using MixSIAR, and to determine dominant source waters during the pre-, peak-, and post-growing seasons. The variations in source water contributions from MixSIAR analysis provided insights into water movement throughout Burstall Wetland at different stages of the growing season. Overall, we found that the seasonal patterns in Burstall Wetland water isotopic rations deviated from expectations during the pre-growing season, reflecting a greater reliance on rainfall than snowmelt, then conformed to expectations during the peak- and post- growing seasons reflecting greater reliance on rainfall, then mixing between groundwater and stream water. The results from this study are important because subalpine wetlands are potentially sensitive to climate change, and it is not yet clear how climate trends will affect source water composition.

4.1 Differences in Spatiotemporal Water Sources Within Burstall Wetland

Stable isotope analysis of $\delta^{18}O$, $\delta^{2}H$, and calculated d-excess in combination with MixSIAR results provides insights into water origins and relative contributions of the Burstall Wetland source waters to downstream water bodies. Plotted rain data followed an expected seasonal distribution, consistent with low temperatures during the pre-growing season, and warmer temperatures during late August and September. The range of depleted to enriched isotopic values of precipitation events are attributed to seasonal changes in the meteorology and moisture sources of the region as easterly up-slope conditions prevail, resulting in mixing of air masses at higher elevations. This is evident in Figure 5 as the progressive enrichment of $\delta^{18}O$ from the pre- to post- growing season is consistent with a rise in temperatures.

D-excess in precipitation defines offsets in δD from the GMWL since values that fall on the GMWL have a *d* of 10‰ by definition (Welp et al., 2012). Thus, if the source of precipitation changes seasonally based on the LMWL, we should expect rain d-excess to follow a seasonal pattern with low d-excess in the summer and high d-excess in the winter (Kondoh and Shimada, 1997). Notably, this process is independent of any surface evaporation since the LMWL only integrates atmospheric processes and not post-precipitation modifications at the land surface. Our results follow this pattern as d-excess decreases from the pre- to post- growing season suggesting rainfall is subjected to increased evaporation effects throughout the growing season. Lone et al. (2021) reported similar results from a high elevation glacier-fed basin in which seasonal changes in isotopic composition of rain were largely controlled by local meteorology and microclimates within the sub-basins.

The isotopic composition of groundwater varied throughout the growing season, both spatially and temporally. The depleted signatures during the pre-growing season are attributed to infiltration and mixing of meltwaters from higher elevations in the Burstall Valley, and from runoff from surrounding uplands. Regardless, the groundwater samples fall between precipitation (rain and snow) indicating that these are major sources of groundwater recharge for Burstall

Wetland. At the end of the peak growing season groundwater d-excess dropped below rainwater coinciding with a period of little to no precipitation and high temperatures, suggesting that water loss occurs from evaporation impacts to a depth of 1 m, triggering a decline in the water table. However, because data points do not fall on the LEL, even when delta values are high, it is difficult to distinguish true evaporative influence on groundwaters. Results also showed considerable spatial variation of the $\delta^{18}O$ content within the wetland. The margins of Burstall Wetland support brown moss and *Equisetum hyemale* (horsetail) and are the first areas to dry during summer months, while the interior mainly supports densely packed shrubs and grasses that remain reasonably wet during summer months. Groundwater $\delta^{18}O$ values are the most depleted at the wetland edges, which may be associated with enhanced evaporative effects to a depth of 1 m however. Although the exact causation for the variations in groundwater $\delta^{18}O$ cannot be uniquely distinguished, the negative influence of vegetation on evaporation because of solar radiation interception is well documented in literature (Zhai et al., 2019; Thompson et al., 2015; Beidermen et al., 2014). Zhai et al. (2019) reported that the spatial distribution of evaporation loss in a shallow wetland was found to be significantly related to vegetation coverage; surface water was shown to have lower evaporative loss in areas of high vegetation coverage compared with areas of low coverage. In a different geographical context, Thompson et al. (2015) found that the rapid regrowth of shrub canopy following a fire event effectively shaded a peatland in the dry Boreal Plains, reducing evaporation at the surface.

Interestingly, the $\delta^{18}O$ composition of stream water remained fairly linear throughout the growing season compared to groundwater and was consistently more depleted, however, the range of d-excess values varied more in streams, yet remained near or slightly above the GMWL, especially during the pre- and post- periods The relatively depleted $\delta^{18}O$ signatures from Stream 2 compared to Stream 1 could indicate a greater degree of surface evaporation from Stream 1 however, even though the range of Stream 2 d-excess values do widen during the post-growing season, they largely remain >10‰. Thus, this trend could be explained by highly depleted water along the LMWL since it crosses the GMWL, and below that point d-excess is greater than 10‰. The consistently depleted stream measurements and highly variable d-excess values draw several possible explanations. First, there are stream measurements that are more depleted than precipitation inputs during the post-growing seasons indicating there is likely a missing low delta end-member since. Glacial meltwater is known to be isotopically depleted in $\delta^{18}O$, thus contributing waters enriched in $\delta^{16}O$ to downstream water bodies (Boral et al., 2019; Gao et al., 2021). Second, the depleted stream water values could be indicative of groundwater sampling limitations since groundwater was only sampled to a depth of 1 m. Deep groundwater (> 1 m in depth) that is mobilized to streams during the post growing season would likely be more depleted in $\delta^{18}O$, thus explaining the depleted stream measurements compared to groundwater, especially in Stream 2 since the average $\delta^{18}O$ is comparable throughout the growing season.

The damped variability of signals within Stream 1 between the pre- and peak- growing seasons indicate mixing and is consistent with results from other studies (Ala-aho et al., 2018; Cao et al., 2018; Lone et al., 2021). Jin et al. (2012) reported similar results from a study conducted in the American Rocky Mountains of seemingly unaffected stream water isotopic composition at the time of snowmelt, when snowmelt presumably provided much of the stream water. They hypothesized that rapid snowmelt releases water with homogenized isotopic value, regardless of stratification during the winter due to increasingly enriched snow fall (Jin et al., 2012). At Burstall, a similar situation could have occurred in which rain on snow events caused mixing, resulting in homogenized waters in streamflow. Indeed, studies confirm that the isotopic composition of precipitation affects that of snowpack outflow and is largely controlled by residence time of liquid water in snowpack (Rücker et al., 2019; Juras et al., 2016). Thus, high magnitude precipitation events occurring during the late spring could cause prolonged residence times and lead to mixing between rain and snow and eventually stream water, creating the resulting damped isotopic values found in this study. However, the effects of rain on snow events are highly variable and further investigation is needed to confirm.

4.2 Relative Source Water Partitioning

Stable water isotopes of $\delta^{18}O$ and $\delta^{2}H$ were used as environmental tracers to determine subalpine source water partitioning during three periods in the growing season (pre-, peak-, post-) using MixSIAR. In general, groundwater via snowmelt was an important water source for all lakes, especially during the pre- growing season. Contributions of snowmelt to groundwater, in addition to streams, created considerable mixing in downstream surface waters. The estimated proportion of rain was greater in all downstream bodies during the pre- and post- growing seasons, coinciding with high precipitation events, suggesting rain was readily mobilized once it reached the surface. Although cooler temperatures during the pre-growing season transition period clearly affected rain signals because they were still reasonably depleted. The posterior density plots do, however, show large uncertainty intervals as to the exact contribution of rain and groundwater during the pre-growing season. The Burstall Lake Outlet and Mudlake posterior plots are multimodal, and the Lake 1 Outlet posterior plot is trimodal, which is the result of a relatively high likelihood of multiple scenarios. Thus, the model creates an output to reflect alternative scenarios. This could be a result of the range in rain and groundwater source data however, outlier analysis did not reveal any outstanding measurements. To address this, informative priors can help when variability among inputs is not sufficient to identify unimodal posterior distributions, or more consumer or tracer data could be added (Moore and Semmens, 2008).

The three sampling periods were able to highlight the progression of water uses to downstream water bodies throughout the growing season. Rain was the dominant driver of streamflow generation during the pre- and peak-growing season in Burstall Wetland after snowmelt inputs declined. All posterior plots of source water estimate that the true portion of rain is falls between 60%-70%, except Lake 1 Outlet. The Lake 1 Outlet posterior plot indicates the true portion of rainwater is slightly higher at 83.2%. The clear period of low rain precipitation during the peak growing season is concerning given the projected occurrence of earlier onsets of spring snowmelt. Longer growing season times may increase evaporation from wetland surface water and groundwater, resulting in a larger summertime water table drop, and greater reliance on rain to stimulate downstream flow.

The post-growing season results indicated that downstream surface waters were largely comprised of groundwater and stream water. The relative contribution of rainwater decreased substantially during this period The increased influx of stream water to downstream water bodies could be a result of high flow rates, supplied by glacial meltwater, since it is well known that meltwater runoff from glaciers, including contributions from both the overlying seasonal snowpack and glacier ice, drives runoff in the eastern Canadian Rockies during the post-growing season (Marshall et al., 2011). In this system, temporal variations of source water proportions were clearly dependent on precipitation inputs during the early and into peak-growing season and a missing low end-member source (we hypothesize glacial meltwater) during the post growing season. Similar to other studies conducted in glacial fed, headwater systems, if glacial mass continues to decline as it has in the past several decades, streamflow in the Burstall Valley may decline during critical times, potentially hindering wetland function as a carbon sink (Cable et al., 2011; Mark and Seltzer, 2003).

4.3 Limitations

The contribution of glacier meltwater was not explicitly considered in this study. This could influence MixSIAR computations of post-growing season calculations since the Robertson Glacier is an integral component of the Burstall Valley hydrology (Beirele et al., 2018). Beirele et al. (2018) reported that meltwater to surface waters is the only major inflow for Lake 2 since Burstall Lake and Lake 1 function as sedimentary traps constraining the movement of groundwater. On a regional scale, glaciers in the greater Bow River Valley were estimated to contribute only 1.8% of the average annual discharge in the Bow River in Banff National Park over a period from 1951-1993 (excluding snowmelt) (Marshall et al., 2013). However, snowmelt contributions are highly variable and site specific depending on snowpack, the amount of rainfall, and the glacier mass balance in a given year, therefore an individualized study of the Burstall Valley is needed to estimate the exact proportion on glacier meltwater reaches the Burstall Wetland. Glacier area is also decreasing in the eastern Rockies so hot, dry summers may no longer produce as large a fraction of glacial meltwater to downstream bodies.

The quantity of snow samples collected in this study were sparse. The relatively enriched signals of snow during the pre-growing season are likely a result of progressive seasonal isotopic enrichment that snowpacks undergo during the melting process (Taylor et al., 2001). The importance of snow and snowmelt, however, is heavily documented in the Canadian Rocky Mountains (Fang et al., 2013; Mercer, 2018; Pomeroy et al., 2016; Hrach et al., 2021; Hayashi et al., 2014). In glacier-fed catchments of the Canadian Rockies, streams originate from glacial meltwater and snow that recharges aquifers during late spring (Penna et al., 2013). In wetlands, this snowmelt provides the primary source that replenishes surface water, recharges groundwater, and contributes to downstream contributions during the spring months. Melt from the seasonal snowpack is known to be the main contributor of streamflow in the eastern slopes of the Canadian Rockies (Fang and Pomeroy, 2020) and should be emphasized in future studies.

5. CONCLUSIONS

There is mounting evidence that wetland hydrological processes in headwater catchments are changing, however, the implications for source water composition are not yet clear (Klein et al., 2005; Lee et al., 2015; Zhang et al., 2016). This research addressed the importance of wetlands in mountain hydrologic systems as potential contributors to downstream water bodies, and the processes that influence them across spatiotemporal scales. Using a stable isotope approach our results revealed significant mixing between source waters during the pre-growing season, indicating that both rain and snow are important components of recharge in the Burstall Valley. The importance of snow meltwater as a driver of streamflow generation is widely recognized however, continued warming is projected to alter pre-growing season snow precipitation regimes. Recent studies have linked patterns of earlier spring snowmelt and amplified rain events in mountain catchments to increased warming (Lopez-Moreno et al., 2021; Musselman et al., 2018; Harpold et al., 2017). These occurrences trigger rain-on-snow events, which are responsible for many of the most damaging floods in mountain areas (Pomeroy et al., 2016). In late June of 2013, rapid snowmelt and heavy rainfall triggered flooding throughout much of the southern half of Alberta (Pomeroy et al., 2016). Tributaries to the Bow River, including the Kananaskis, reached flood levels, and wetlands in this region eventually became overwhelmed leading to some damage. Although it is impossible to estimate the exact benefits wetlands provide during such events, it is important to continue to re-evaluate and study ecosystem hydrologic response to best prepare for the future flood events.

During the peak growing seasons, wetlands in snow-dominated landscapes are experiencing earlier drawdowns, accelerated recession rates, and lower minimum water levels as snowpack declines initiate earlier runoff (Ray et al., 2019). This leads to longer growing seasons resulting in greater reliance on rain and presumably, glacial meltwater to maintain downstream flow. Under these circumstances, consecutive years of drought could put Burstall at risk of significant water loss due to longer growing seasons and increased evaporation rates. This is true for other subalpine headwater catchments that may experience similar shifts in hydrological processes due to continued environmental change.

ACKNOWLEDGEMENTS

We would like to thank our funding partners, Canada First Research Excellence Fund, Global Water Futures, Mountain Water Futures Program, Alberta Innovates, and Natural Science and

Engineering Research Council of Canada Discovery and CREATE grants programs for the financial support on research conducted within this project. Thank you to Sheryl Chau and Yi Abby Wang for their assistance in data collection during the summers of 2019 and 2020. Finally, thank you to Matt Bolding, Calvin Lei, and Jordan Reynolds from the Rooney Lab (University of Waterloo) for conducting the vegetation survey and sharing raw data and to Cherie Westbrook (University of Saskatchewan) for sharing isotope data.

DATA AVAILABILITY

The data presented in this study are available upon reasonable request from the corresponding author.

REFERENCES

Ala-Aho, P., Soulsby, C., Pokrovsky, O. S., Kirpotin, S. N., Karlsson, J., Serikova, S., ... & Tetzlaff, D. (2018). Using stable isotopes to assess surface water source dynamics and hydrological connectivity in a high-latitude wetland and permafrost influenced landscape. *Journal of Hydrology*, 556, 279-293.

Beierle, B. D., Smith, D. G., & Hills, L. V. (2003). Late quaternary glacial and environmental history of the Burstall Pass area, Kananaskis Country, Alberta, Canada. *Arctic, Antarctic, and Alpine Research*, 35(3), 391-398.

Biederman, J. A., Harpold, A. A., Gochis, D. J., Ewers, B. E., Reed, D. E., Papuga, S. A., & Brooks, P. D. (2014). Increased evaporation following widespread tree mortality limits streamflow response. *Water Resources Research*, 50(7), 5395-5409.

Boral, S., Sen, I. S., Ghosal, D., Peucker-Ehrenbrink, B., & Hemingway, J. D. (2019). Stable water isotope modeling reveals spatio-temporal variability of glacier meltwater contributions to Ganges River headwaters. *Journal of Hydrology*, 577, 123983.

Cable, J., Ogle, K., & Williams, D. (2011). Contribution of glacier meltwater to streamflow in the Wind River Range, Wyoming, inferred via a Bayesian mixing model applied to isotopic measurements. *Hydrological Processes*, 25(14), 2228-2236.

Cao, X., Wu, P., Zhou, S., Han, Z., Tu, H., & Zhang, S. (2018). Seasonal variability of oxygen and hydrogen isotopes in a wetland system of the Yunnan-Guizhou Plateau, southwest China: a quantitative assessment of groundwater inflow fluxes. *Hydrogeology journal*, 26(1), 215-231.

Clay, A., Bradley, C., Gerrard, A. J., & Leng, M. J. (2004). Using stable isotopes of water to infer wetland hydrological dynamics. *Hydrology and Earth System Sciences*, 8(6), 1164-1173.

Colvin, S. A., Sullivan, S. M. P., Shirey, P. D., Colvin, R. W., Winemiller, K. O., Hughes, R. M., ... & Eby, L. (2019). Headwater streams and wetlands are critical for sustaining fish, fisheries, and ecosystem services. *Fisheries*, 44(2), 73-91.

Craig, H. (1961). Isotopic variations in meteoric waters. *Science*, 133(3465), 1702-1703.

Dansgaard, W. (1964). Stable isotopes in precipitation. *tellus*, 16(4), 436-468.

Fang, X., & Pomeroy, J. W. (2020). Diagnosis of future changes in hydrology for a Canadian Rockies headwater basin. *Hydrology and Earth System Sciences*, 24(5), 2731-2754.

Fang, X., Pomeroy, J. W., Ellis, C. R., MacDonald, M. K., DeBeer, C. M., & Brown, T. (2013). Multi-variable evaluation of hydrological model predictions for a headwater basin in the Canadian Rocky Mountains. *Hydrology and Earth System Sciences*, 17(4), 1635-1659.

Gao, Z., Weng, H., & Guo, H. (2021). Unraveling influences of nitrogen cycling on arsenic enrichment in groundwater from the Hetao Basin using geochemical and multi-isotopic approaches. *Journal of Hydrology*, 595, 125981.

Gröning, M., Lutz, H. O., Roller-Lutz, Z., Kralik, M., Gourcy, L., & Pöltenstein, L. (2012). A simple rain collector preventing water re-evaporation dedicated for δ18O and δ2H analysis of cumulative precipitation samples. *Journal of Hydrology*, 448, 195-200.

Grusson, Y., Sun, X., Gascoin, S., Sauvage, S., Raghavan, S., Anctil, F., & Sáchez-Pérez, J. M. (2015). Assessing the capability of the SWAT model to simulate snow, snow melt and streamflow dynamics over an alpine watershed. *Journal of Hydrology*, 531, 574-588.

Harpold, A. A., & Kohler, M. (2017). Potential for changing extreme snowmelt and rainfall events in the mountains of the western United States. *Journal of Geophysical Research: Atmospheres*, 122(24), 13-219.

Hayashi, M., & Farrow, C. R. (2014). Watershed-scale response of groundwater recharge to inter-annual and inter-decadal variability in precipitation (Alberta, Canada). *Hydrogeology Journal,* 22(8), 1825-1839.

Hrach, D. M., Green, A., Khomik, M., & Petrone, R. M. (2021). Analysis of growing season carbon and water fluxes of a subalpine wetland in the Canadian Rocky Mountains: implications of shade on ecosystem water use efficiency. *Hydrological Processes*, e14425.

Hrach, D. M. (2020). Quantifying the role of shade on microclimate conditions and water use efficiency of a subalpine wetland in the Canadian Rocky Mountains, Kananaskis, Alberta (Master's thesis, University of Waterloo).

Jin, S. G., Hassan, A. A., & Feng, G. P. (2012). Assessment of terrestrial water contributions to polar motion from GRACE and hydrological models. *Journal of Geodynamics*, 62, 40-48.

Juras, R., Pavlásek, J., Vitvar, T., Šanda, M., Holub, J., Jankovec, J., & Linda, M. (2016). Isotopic tracing of the outflow during artificial rain-on-snow event. *Journal of Hydrology*, 541, 1145-1154.

Katvala, S.M. Isotope hydrology of the upper Bow River basin. Master's Thesis, University of Calgary, Calgary, AB, Canada, 2008.

Klein, E., Berg, E. E., & Dial, R. (2005). Wetland drying and succession across the Kenai Peninsula Lowlands, south-central Alaska. *Canadian Journal of Forest Research*, 35(8), 1931-1941.

KONDOH, A., & SHIMADA, J. (1997). The origin of precipitation in eastern Asia by deuterium excess. *Journal of Japan Society of Hydrology and Water Resources*, 10(6), 627-629.

Langs, L. E., Petrone, R. M., & Pomeroy, J. W. (2020). A δ18O and δ2H stable water isotope analysis of subalpine forest water sources under seasonal and hydrological stress in the Canadian Rocky Mountains. *Hydrological Processes*, 34(26), 5642-5658.

Lee, S. Y., Ryan, M. E., Hamlet, A. F., Palen, W. J., Lawler, J. J., & Halabisky, M. (2015). Projecting the hydrologic impacts of climate change on montane wetlands. *Plos one*, 10(9), e0136385.

Le Maitre DC, Scott DF, Colvin C. 1999. A review of information on interactions between vegetation and groundwater. *Water South Africa* 25:137–52

Lessels, J. S., Tetzlaff, D., Birkel, C., Dick, J., & Soulsby, C. (2016). Water sources and mixing in riparian wetlands revealed by tracers and geospatial analysis. *Water Resources Research*, 52(1), 456-470.

Liu, Y., & Yamanaka, T. (2012). Tracing groundwater recharge sources in a mountain–plain transitional area using stable isotopes and hydrochemistry. *Journal of Hydrology*, 464, 116-126.

Lone, A., Jeelani, G., Deshpande, R. D., & Padhya, V. (2021). Estimating the sources of stream water in snow dominated catchments of western Himalayas. *Advances in Water Resources*, 155, 103995.

López-Moreno, J. I., Pomeroy, J. W., Morán-Tejeda, E., Revuelto, J., Navarro-Serrano, F. M., Vidaller, I., & Alonso-González, E. (2021). Changes in the frequency of global high mountain rain-on-snow events due to climate warming. *Environmental Research Letters*, 16(9), 094021.

Mark, B. G., & Seltzer, G. O. (2003). Tropical glacier meltwater contribution to stream discharge: a case study in the Cordillera Blanca, Peru. *Journal of glaciology*, 49(165), 271-281.

Marshall, S. J., White, E. C., Demuth, M. N., Bolch, T., Wheate, R., Menounos, B., ... & Shea, J. M. (2011). Glacier water resources on the eastern slopes of the Canadian Rocky Mountains. *Canadian Water Resources Journal*, 36(2), 109-134.

Maurya, A. S., Shah, M., Deshpande, R. D., Bhardwaj, R. M., Prasad, A., & Gupta, S. K. (2011). Hydrograph separation and precipitation source identification using stable water isotopes and conductivity: River Ganga at Himalayan foothills. *Hydrological Processes*, 25(10), 1521-1530.

Mengistu, M. G., Everson, C. S., & Clulow, A. D. (2014). The impact of taro (Colocasia esculenta) cultivation on the total evaporation of a Cyperus latifolius marsh. *Hydrological Processes*, 28(3), 620-627.

Mercer, J. J. (2018). Insights into mountain wetland resilience to climate change: An evaluation of the hydrological processes contributing to the hydrodynamics of alpine wetlands in the Canadian Rocky Mountains (Doctoral dissertation, University of Saskatchewan).

Moore, J. W., & Semmens, B. X. (2008). Incorporating uncertainty and prior information into stable isotope mixing models. *Ecology letters*, 11(5), 470-480.

Moran, T. A., Marshall, S. J., Evans, E. C., & Sinclair, K. E. (2007). Altitudinal gradients of stable isotopes in lee-slope precipitation in the Canadian Rocky Mountains. *Arctic, Antarctic, and Alpine Research*, 39(3), 455-467.

Musselman, K. N., Lehner, F., Ikeda, K., Clark, M. P., Prein, A. F., Liu, C., ... & Rasmussen, R. (2018). Projected increases and shifts in rain-on-snow flood risk over western North America. *Nature Climate Change*, 8(9), 808-812.

Penna, D., Mao, L., Comiti, F., Engel, M., Dell'Agnese, A., & Bertoldi, G. (2013). Hydrological effects of glacier melt and snowmelt in a high-elevation catchment. *Die Bodenkultur*, 64(3-4), 93-98.

Pomeroy, J. W., Stewart, R. E., & Whitfield, P. H. (2016). The 2013 flood event in the South Saskatchewan and Elk River basins: Causes, assessment and damages. *Canadian Water Resources Journal/Revue Canadienne Des Ressources Hydriques*, 41(1-2), 105-117.

Pu, T., He, Y., Zhu, G., Zhang, N., Du, J., & Wang, C. (2013). Characteristics of water stable isotopes and hydrograph separation in Baishui catchment during the wet season in Mt. Yulong region, south western China. *Hydrological Processes*, 27(25), 3641-3648.

Ray, A. M., Sepulveda, A. J., Irvine, K. M., Wilmoth, S. K., Thoma, D. P., & Patla, D. A. (2019). Wetland drying linked to variations in snowmelt runoff across Grand Teton and Yellowstone national parks. *Science of the Total Environment*, 666, 1188-1197.

Reynolds, J. N., Swanson, H. K., & Rooney, R. C. (2022). Habitat area and environmental filters determine avian richness along an elevation gradient in mountain peatlands. *Journal of Avian Biology*, 2022(2), e02797.

Rodgers, P., Soulsby, C., Waldron, S., & Tetzlaff, D. (2005). Using stable isotope tracers to assess hydrological flow paths, residence times and landscape influences in a nested mesoscale catchment. *Hydrology and Earth System Sciences*, 9(3), 139-155.

Rücker, A., Boss, S., Kirchner, J. W., & Freyberg, J. V. (2019). Monitoring snowpack outflow volumes and their isotopic composition to better understand streamflow generation during rain-on-snow events. *Hydrology and Earth System Sciences*, 23(7), 2983-3005.

Šanda, M., Vitvar, T., Kulasová, A., Jankovec, J., & Císlerová, M. (2014). Run-off formation in a humid, temperate headwater catchment using a combined hydrological, hydrochemical and isotopic approach (Jizera Mountains, Czech Republic). *Hydrological Processes*, 28(8), 3217-3229.

Scanlon, R. S. (2017). Modeling mass balance at Robertson Glacier, Alberta, Canada 1912-2012 (Doctoral dissertation, Montana State University-Bozeman, College of Letters & Science).

Soulsby, C., Birkel, C., Geris, J., Dick, J., Tunaley, C., & Tetzlaff, D. (2015). Stream water age distributions controlled by storage dynamics and nonlinear hydrologic connectivity: Modeling with high-resolution isotope data. *Water Resources Research*, 51(9), 7759-7776.

Stewart, R. E., Bachand, D., Dunkley, R. R., Giles, A. C., Lawson, B., Legal, L., Miller, S. T., Murphy, B. P., Parker, M. N., Paruk, B. J., and Yau, M. K., (1995): Winter storms over Canada. *Atmosphere-Ocean*, 33(2): 233–247.

Stock, B. C., & Semmens, B. X. (2016). Unifying error structures in commonly used biotracer mixing models. *Ecology*, 97(10), 2562-2569.

Stock and Semmens, 2013 B.C. Stock, B.X. Semmens
MixSIAR GUI User Manual, Version 3.1
http://conserver.iugocafe.org/user/brice.semmens/MixSIAR (2013)

Stock, B. C., Jackson, A. L., Ward, E. J., Parnell, A. C., Phillips, D. L., & Semmens, B. X. (2018). Analyzing mixing systems using a new generation of Bayesian tracer mixing models. *PeerJ*, 6, e5096.

Taylor, S., Feng, X., Kirchner, J. W., Osterhuber, R., Klaue, B., & Renshaw, C. E. (2001). Isotopic evolution of a seasonal snowpack and its melt. *Water Resources Research*, 37(3), 759-769.

Thompson, D. K., Baisley, A. S., & Waddington, J. M. (2015). Seasonal variation in albedo and radiation exchange between a burned and unburned forested peatland: implications for peatland evaporation. *Hydrological Processes*, 29(14), 3227-3235.

Welp, L. R., Lee, X., Griffis, T. J., Wen, X. F., Xiao, W., Li, S., ... & Huang, J. (2012). A meta-analysis of water vapor deuterium-excess in the midlatitude atmospheric surface layer. *Global Biogeochemical Cycles*, 26(3).

Whitfield, P. H. (2014). Climate station analysis and fitness for purpose assessment of 3053600 Kananaskis, Alberta. *Atmosphere-Ocean*, 52(5), 363-383.

Windell, J. T., & Segelquist, C. (1986). An ecological characterization of Rocky Mountain montane and subalpine wetlands (Vol. 86, No. 11). Fish and Wildlife Service, US Department of the Interior.

Wu, Y., Zhang, G., & Rousseau, A. N. (2020). Quantitative assessment on basin-scale hydrological services of wetlands. *Science China Earth Sciences*, 63(2), 279-291.

Wu, H., Wu, J., Song, F., Abuduwaili, J., Saparov, A. S., Chen, X., & Shen, B. (2019). Spatial distribution and controlling factors of surface water stable isotope values (δ18O and δ2H) across Kazakhstan, Central Asia. *Science of the Total Environment*, 678, 53-61.

Zhai, L., Wang, X., Wang, P., Miralles-Wilhelm, F., & Sternberg, L. D. S. L. (2019). Vegetation and location of water inflow affect evaporation in a subtropical wetland as indicated by the deuterium excess method. *Ecohydrology*, 12(4), e2082.

Zhang, Q., Knowles, J. F., Barnes, R. T., Cowie, R. M., Rock, N., & Williams, M. W. (2018). Surface and subsurface water contributions to streamflow from a mesoscale watershed in complex mountain terrain. *Hydrological processes*, 32(7), 954-967.

Zhang, W., Yi, Y., Song, K., Kimball, J. S., & Lu, Q. (2016). Hydrological response of alpine wetlands to climate warming in the eastern Tibetan Plateau. *Remote Sensing*, 8(4), 336

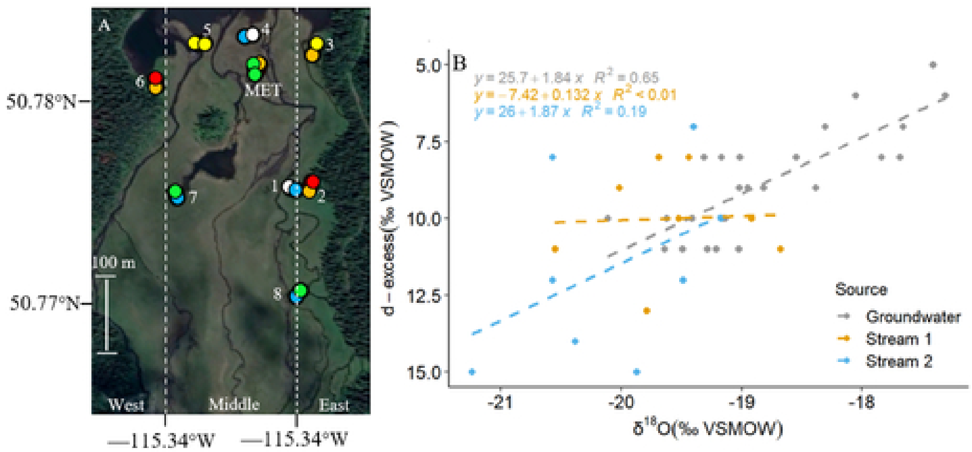

44x20mm (300 x 300 DPI)

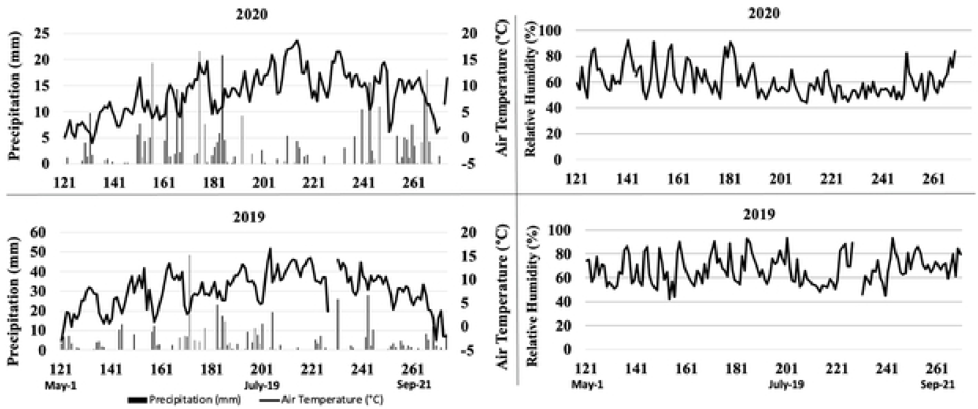

53x22mm (300 x 300 DPI)

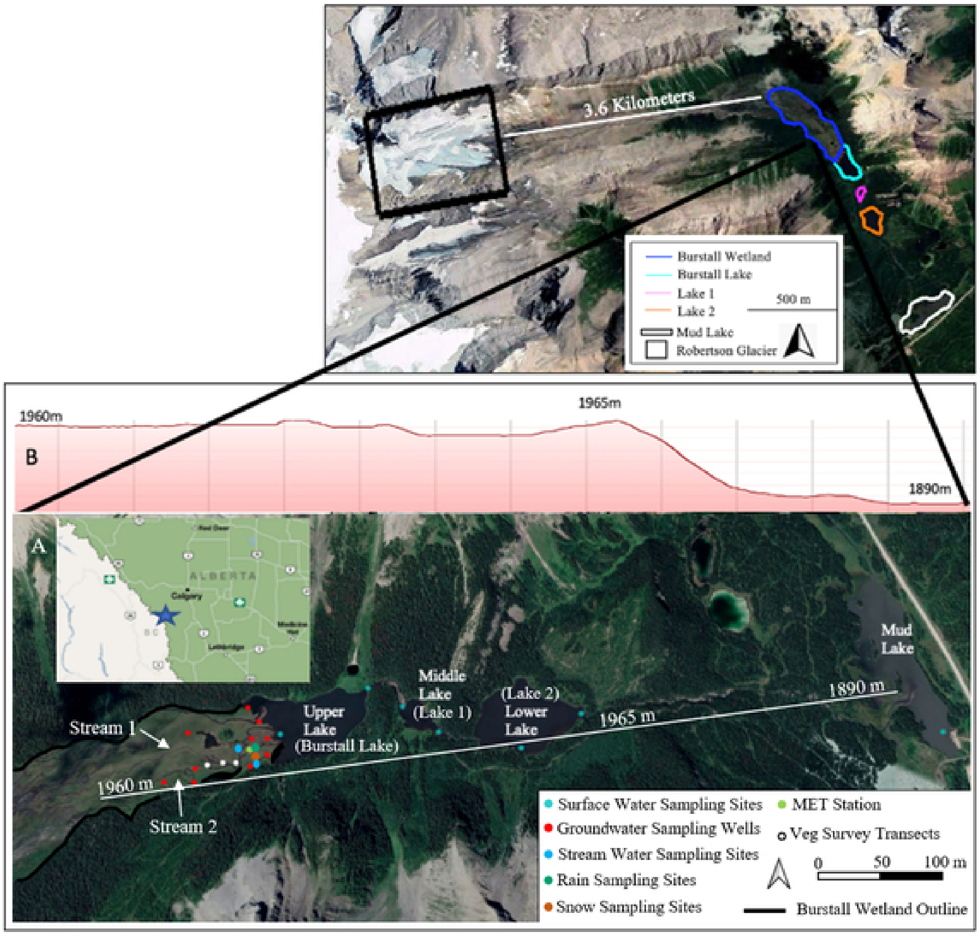

49x46mm (300 x 300 DPI)

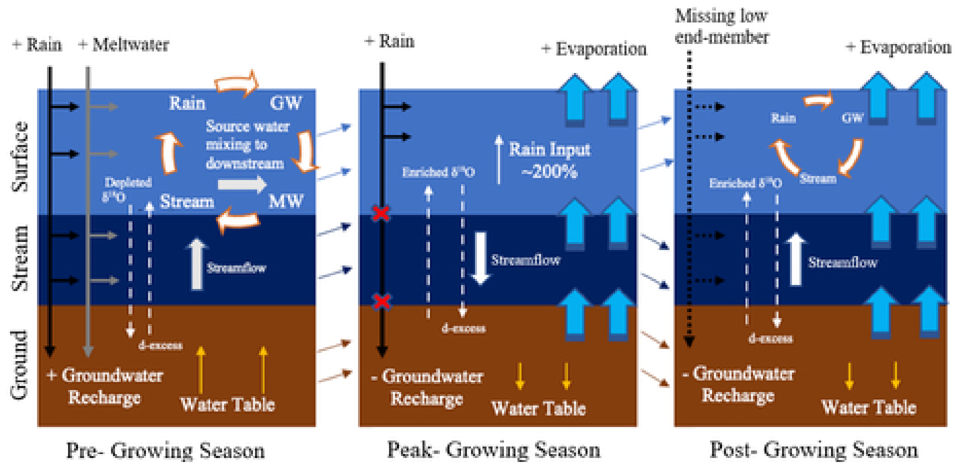

43x20mm (300 x 300 DPI)

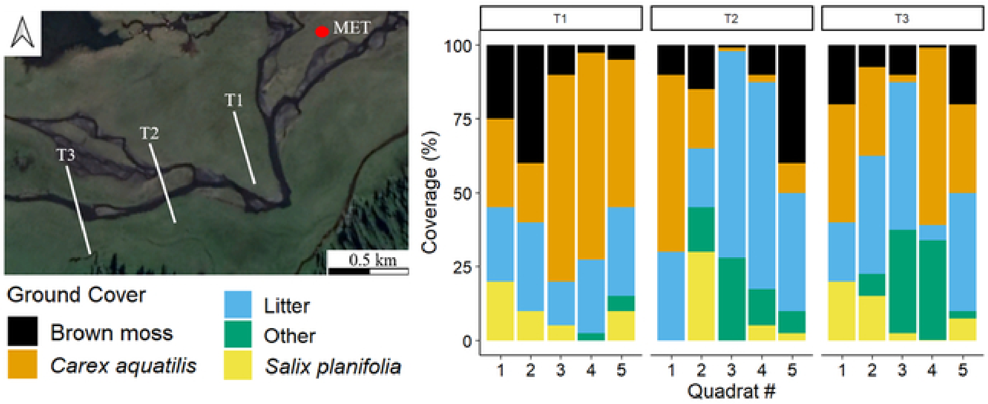

55x23mm (300 x 300 DPI)

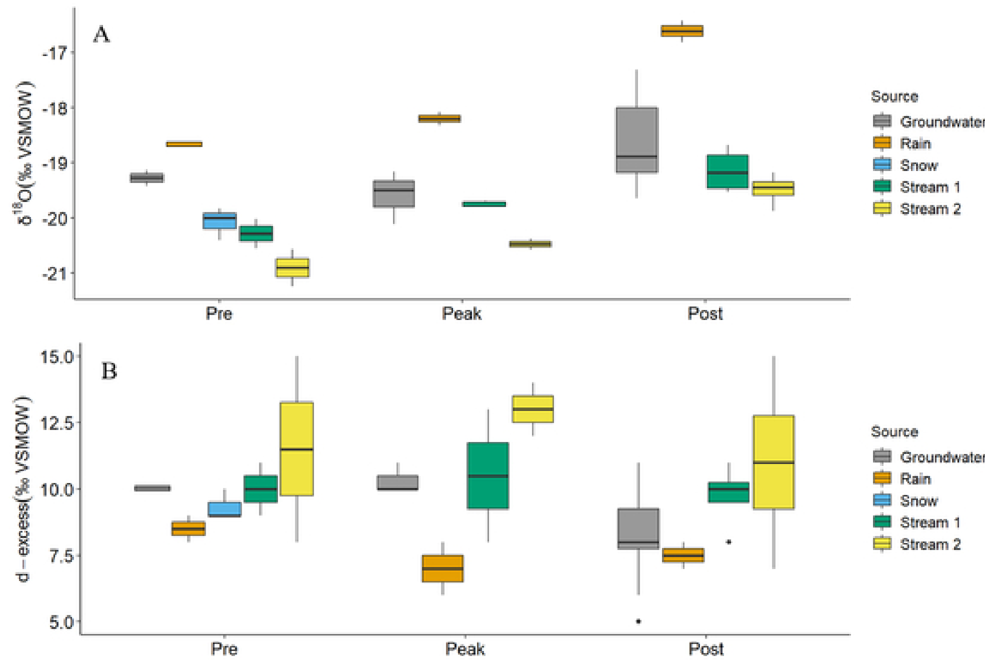

49x33mm (300 x 300 DPI)

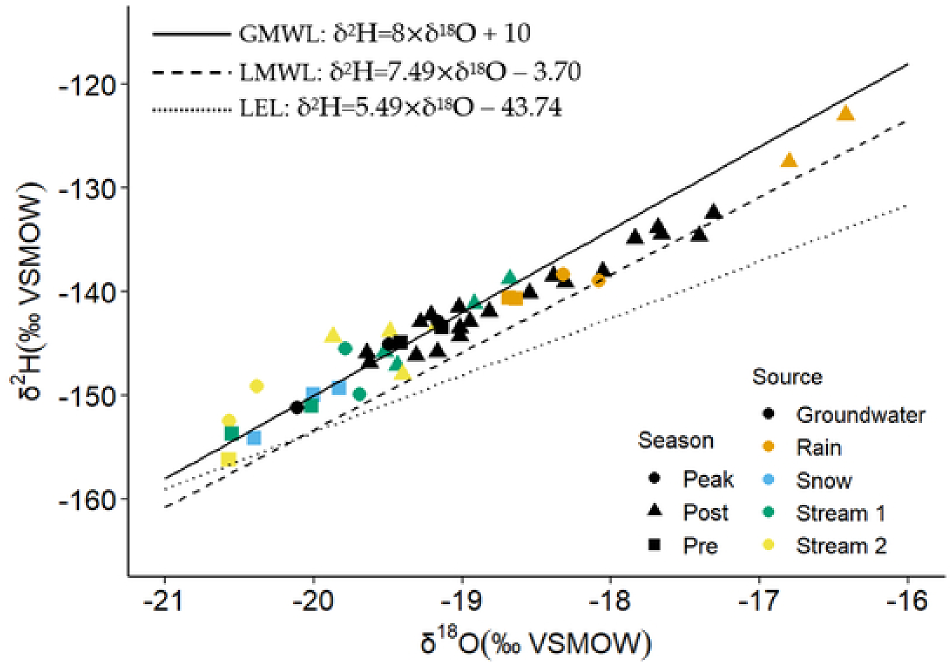

48x32mm (300 x 300 DPI)

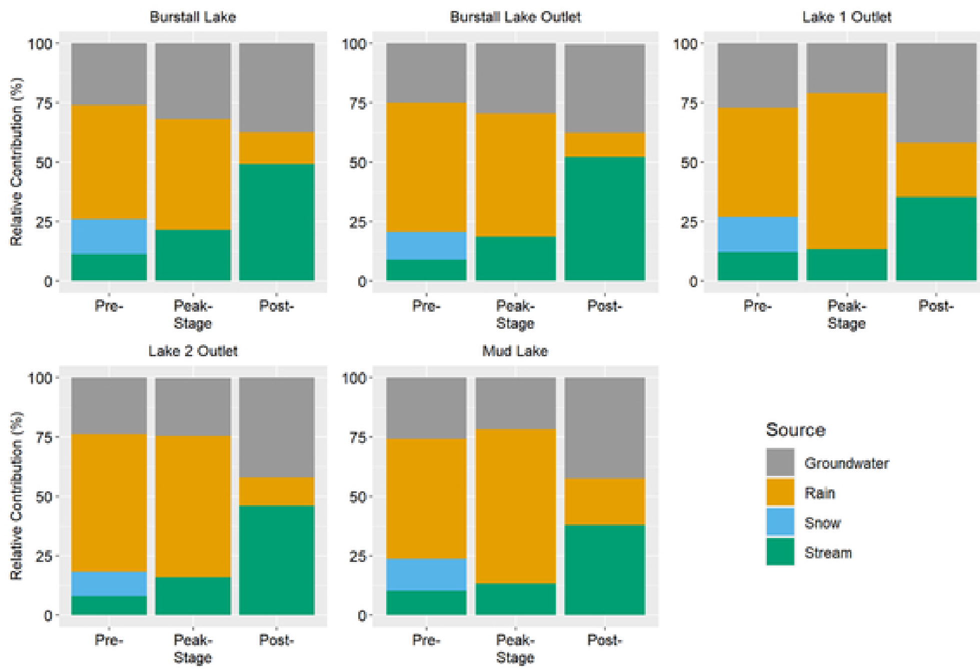

48x32mm (300 x 300 DPI)

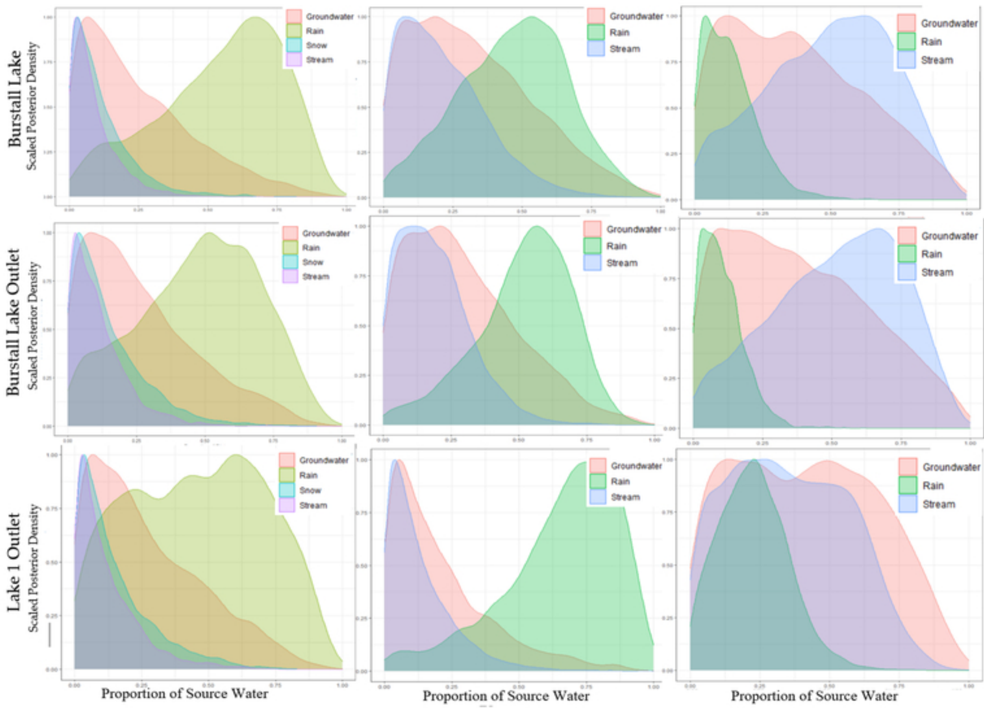

65x47mm (300 x 300 DPI)

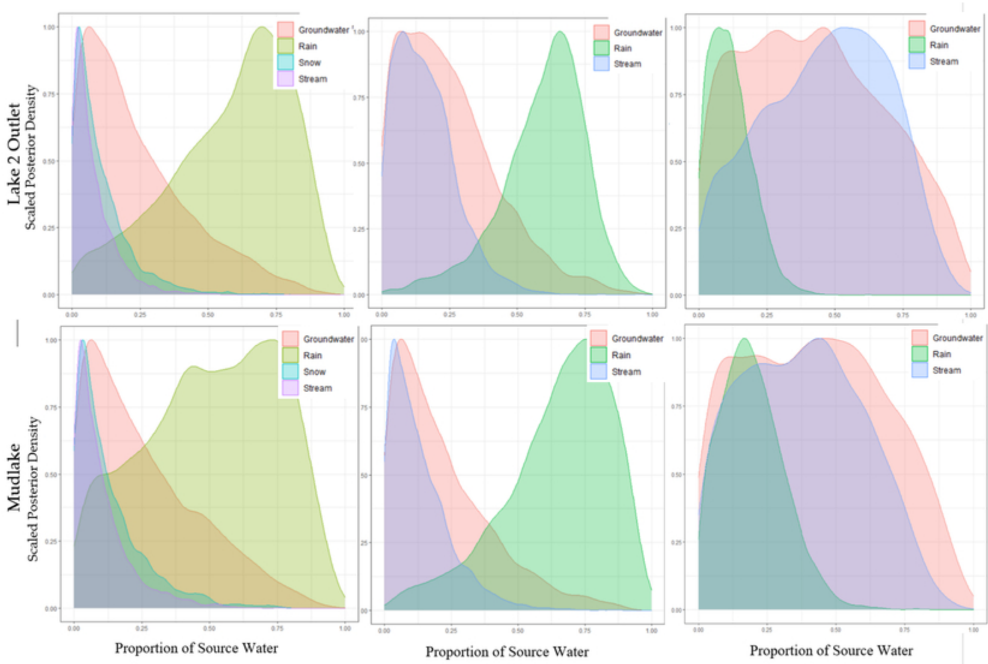

70x47mm (300 x 300 DPI)

		Average		
		δ18O	**δ2H**	**d-excess**
Pre-	Groundwater	-19.2	-144.1	10.0
	Stream 1	-20.2	-152.3	10.0
	Stream 2	-20.9	-155.5	11.5
	Rain	-18.6	-140.6	8.0
	Snow	-20.0	-151.1	9.3
Peak-	Groundwater	-19.5	-146.4	10.3
	Stream 1	-19.7	-147.7	10.5
	Stream 2	-20.4	-150.7	13.0
	Rain	-18.2	-138.6	7.0
Post-	Groundwater	-18.6	-140.4	8.4
	Stream 1	-19.1	-143.2	9.7
	Stream 2	-19.4	-144.8	11.0
	Rain	-15.2	-114.9	6.7